

PCCP

Accepted Manuscript



This article can be cited before page numbers have been issued, to do this please use: D. S. N. Parker, R. I. Kaiser, O. Kostko, T. Troy, M. Ahmed, B. J. Sun, S. H. Chen and A. H. Chang, *Phys. Chem. Chem. Phys.*, 2015, DOI: 10.1039/C5CP02960K.



This is an *Accepted Manuscript*, which has been through the Royal Society of Chemistry peer review process and has been accepted for publication.

Accepted Manuscripts are published online shortly after acceptance, before technical editing, formatting and proof reading. Using this free service, authors can make their results available to the community, in citable form, before we publish the edited article. We will replace this *Accepted Manuscript* with the edited and formatted *Advance Article* as soon as it is available.

You can find more information about *Accepted Manuscripts* in the [Information for Authors](#).

Please note that technical editing may introduce minor changes to the text and/or graphics, which may alter content. The journal's standard [Terms & Conditions](#) and the [Ethical guidelines](#) still apply. In no event shall the Royal Society of Chemistry be held responsible for any errors or omissions in this *Accepted Manuscript* or any consequences arising from the use of any information it contains.

On the Formation of Pyridine in the Interstellar Medium

Dorian S. N. Parker, Ralf. I. Kaiser*

Department of Chemistry, University of Hawaii at Manoa, Honolulu, HI 96822, USA

Oleg Kostko, Tyler P. Troy, Musahid Ahmed*

Chemical Sciences Division, Lawrence Berkeley National Laboratory, Berkeley, CA 94720, USA

Bing-Jian Sun, Shih-Hua Chen, A. H. H. Chang*

Department of Chemistry, National Dong Hwa University, Shoufeng, Hualien 974, Taiwan

Abstract

Nitrogen-substituted polycyclic aromatic hydrocarbons (NPAHs) have been proposed to play a key role in the astrochemical evolution of the interstellar medium, but the formation mechanism of even their simplest building block - the aromatic pyridine molecule – has remained elusive for decades. Here we reveal a potential pathway to a facile pyridine (C_5H_5N) synthesis via the reaction of the cyano vinyl (C_2H_2CN) radical with vinyl cyanide (C_2H_3CN) in high temperature environments simulating conditions in carbon-rich circumstellar envelopes of Asymptotic Giant Branch (AGB) stars like IRC+10216. Since this reaction is barrier-less, pyridine can be also synthesized via this bimolecular reaction in cold molecular clouds such as in TMC-1. The synchronized aromatization of precursors readily available in the interstellar medium leading to nitrogen incorporation into the aromatic rings would open up a novel route to pyridine derivatives such as vitamin B3 and pyrimidine bases as detected in carbonaceous chondrites like Murchison.

Keywords: ISM: molecules, molecular processes, astrochemistry, methods: laboratory: molecular

1. Introduction

Carbonaceous chondrites such as the Murchison meteorite contain a unique chemical record of the early Solar System.¹ Often dubbed as primordial fossils, carbonaceous chondrites carry biorelevant molecules such as vitamins (vitamin B3, niacin)² and nucleobases (pyrimidines, purines).^{3, 4} These species contain the structural motif of pyridine the simplest nitrogen-bearing aromatic molecule (C_5H_5N).⁵ The detection of terrestrially rare nucleobases 2,6-diaminopurine and 6,8-diaminopurine in Murchison^{3, 6} together with an $^{15}N/^{14}N$ isotope enrichment⁷ suggest an interstellar origin. Pyridine also represents the key building block of nitrogen-substituted polycyclic aromatic hydrocarbons (NPAHs) like quinoline, implicated to be ubiquitous in the interstellar medium with overall contributions of a few 10 % to the cosmic carbon budget.⁸ Circumstellar envelopes (CSEs) of carbon-rich Asymptotic Giant Branch (AGB) stars like IRC+10216, where temperatures range up to a few 1,000 K close to the photosphere of the central star,⁹⁻¹¹ are believed to be the ultimate breeding grounds of nitrogen substituted polycyclic aromatic hydrocarbons. Current astrochemical models propose that the synthesis of the simplest building block of NPAHs - the aromatic pyridine molecule (C_5H_5N) - is driven by radical mediated reactions of hydrogen cyanide (HCN) with acetylene (C_2H_2).¹² However, these mechanisms have not been verified experimentally. A recent study proposed pyridine formation via methylidyne radical (CH) insertion into pyrrole (C_4H_5N),¹³ but even pyrrole has never been detected in the interstellar medium. Hence, the formation of interstellar pyridine has remained elusive to date.

Here, we provide compelling evidence that the aromatic pyridine molecule (C_5H_5N) is formed via the gas phase reaction of the cyano vinyl (C_2H_2CN) radical with vinyl cyanide (C_2H_3CN) at temperatures of 1,000 K characteristic of circumstellar envelopes of carbon stars. Since this reaction is barrier-less, pyridine can be also synthesized in cold molecular clouds such as in TMC-1. This reaction is the simplest representative of a whole new reaction class in which nitrogen-substituted aromatic molecules with a pyridine core can be synthesized from readily available acyclic precursors. Here, the precursors vinyl cyanide^{14, 15} together with its radical derivatives reside in circumstellar envelopes of carbon-rich stars such as of IRC+10216 and also in cold molecular clouds like TMC-1.

2. Experimental

The experiments were carried out at the Advanced Light Source (ALS) at the Chemical Dynamics Beamline (9.0.2.) utilizing a 'pyrolytic reactor', which consists of a resistively heated silicon carbide nozzle at a temperature of 1000 ± 100 K. The temperature of the SiC tube was monitored using a Type-C thermocouple, the distance between the electrodes was 20 mm, and 2 A and 16 V were applied to generate 32 W. Phenyl radicals (C_6H_5) were generated *in situ* via quantitative pyrolysis of helium-seeded nitrosobenzene (C_6H_5NO ; Aldrich; 99.5 %+) at a backing pressure of 300 Torr. This mixture was then mixed with vinyl cyanide (C_2H_3CN ; Aldrich; 99.9 %+). The phenyl radicals were generated at concentrations of less than 0.1 %; vinyl cyanide concentrations were held at 0.9 %. Cyanovinyl radicals (C_2H_2CN) were likely generated *in situ* via hydrogen abstraction from vinyl cyanide (C_2H_3CN) at the α -carbon atom by the phenyl radical (C_6H_5). After exiting the pyrolytic reactor, the molecular beam passes a skimmer and enters a detection chamber containing a Wiley–McLaren Reflectron Time-of-Flight (ReTOF) mass spectrometer. The products were photoionized in the extraction region of the spectrometer by exploiting quasi continuous tunable vacuum ultraviolet (VUV) light from the Chemical Dynamics Beamline 9.0.2 of the Advanced Light Source and detected with a microchannel plate (MCP) detector. Here, a mass spectrum was taken in 0.05 eV intervals from 8.00 eV to 10.00 eV. The photoionization efficiency (PIE) curves were generated by integrating the signal collected at a specific mass-to-charge ratio (m/z) selected for the species of interest over the range of photon energies in 0.05 eV increments and normalized to the incident photon flux.

3. Theoretical Methods

Our electronic structure calculations were conducted at a level of theory that could predict relative energies of the intermediates, transition states, and products of the reactions of vinyl cyanide with the vinyl and cyanovinyl radical to an accuracy of about 15 kJ mol^{-1} .⁵²⁻⁵⁴ Stationary points were optimized at the hybrid density functional B3LYP level with the cc-pVTZ basis set.¹⁶⁻¹⁹ Vibrational frequencies were calculated using the same B3LYP/cc-pVTZ method and were used to compute zero-point vibrational energy (ZPE) corrections. Relative energies of these species were refined employing the CCSD(T)/cc-pVTZ method²⁰⁻²² including ZPEs obtained by B3LYP calculations. Rice–Ramsperger–Kassel–Marcus (RRKM) theory was exploited to predict the branching ratios for the vinyl plus vinylcyanide and cyanovinyl plus vinylcyanide reactions

shown in the supporting information.³¹ Optimized Cartesian coordinates (in Å) of various intermediates, transition states, and products are compiled in the Figure 5. The validity of present theoretical method (B3LYP/cc-pVTZ geometry//CCSD(T)/cc-pVTZ energy) is assessed by taking the transition state between i6 and i8 (Figures 4 and 5) as an example. When a larger basis set with diffuse functions (aug-cc-pVTZ) is employed, the costly B3LYP/aug-cc-pVTZ//CCSD(T)/aug-cc-pVTZ gives an energy of -6 kJ mol⁻¹ for this transition state; while multiconfiguration CCSD/cc-pVDZ optimized geometry yields an energy at the CCSD(T)/cc-pVTZ level of -1 kJ mol⁻¹. The assessment supports that the choice of the present level of calculations is sensible.

4. Experimental Results

The formation of pyridine was studied experimentally in a 'pyrolytic reactor', which consists of a resistively heated silicon carbide nozzle at a temperature of 1000 ± 100 K.²³ Figure 1 depicts a characteristic mass spectrum recorded at 10.00 eV photoionization energy with products detected at mass-to-charge ratios from m/z 15 to m/z 129. These are m/z 15 (CH_3^+), 52 (C_4H_4^+), 65 (C_5H_5^+), 78 (C_6H_6^+), 79 ($\text{C}_5\text{H}_5\text{N}^+$), 103 ($\text{C}_7\text{H}_5\text{N}^+$), 104 (C_8H_8^+), and 129 ($\text{C}_9\text{H}_7\text{N}^+$). We shift our attention now to the identification of the product isomer(s) formed based on an analysis of the photoionization efficiency (PIE) curves, which report the intensities of the ions as a function of photon energy (Figure 2). The PIE curve at m/z 129 was matched with a reference PIE of cinnamon nitrile ($\text{C}_6\text{H}_5\text{CHCHCN}$), i.e. α -cyanostyrene. The PIE at m/z 104 could be fit with a linear combination of the reference PIEs of styrene ($\text{C}_6\text{H}_5\text{C}_2\text{H}_3$)²⁴ and ¹³C-benzonitrile (¹³CC₅H₅CN/ $\text{C}_6\text{H}_5^{13}\text{CN}$).²⁵ It is important to stress that 1,4-dicyano-1,3-butadiene (104 u) cannot be probed experimentally. Here, the ionization energy of 1,4-dicyano-1,3-butadiene ranges between 9.9 eV and 10.1 eV; therefore, close to the ionization threshold, little ion signal – if at all – is expected to contribute to the ion counts at $m/z = 104$. The PIE at m/z 103 is fit solely with the benzonitrile ($\text{C}_6\text{H}_5\text{CN}$) PIE.²⁵ Note that the PIE at m/z 79 could only be fit only with the reference PIE of pyridine ($\text{C}_5\text{H}_5\text{N}$).²⁵ The PIE curves derived from signals at lower masses were found to originate from hydrocarbons and their radicals: benzene (m/z 78; C_6H_6),²⁶ cyclopentadienyl (m/z 65; C_5H_5),²⁷ vinylacetylene (m/z 52; C_4H_4),²⁶ and the methyl radical (m/z 15; CH_3).²⁸ We would like to stress that PIEs of aromatic molecules compared to their acyclic isomers differ drastically by their shape and also in their ionization energy.^{24, 29} Therefore, within

the limit of our data, pyridine alone fits the experimental data exceptionally well; there is no other aromatic isomer of the molecular formula C_5H_5N . It should be noted that the isomers identified above denote all the products formed in the reaction of phenyl radicals with vinyl cyanide. The universal nature of VUV mass spectrometry means no structure or molecule is undetectable. With the high sensitivity of this detection method, systems studied so far have had all the molecules identified, both intermediates and products.

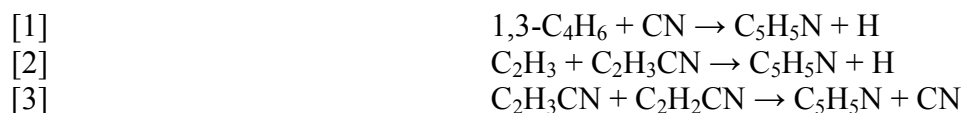
5. Discussion

Having identified the products, we are proposing now the underlying reaction pathways to the nitrogen-bearing products cinnamon nitrile ($C_6H_5CHCHCN$), benzonitrile (C_6H_5CN), and pyridine (C_5H_5N) and expand these considerations to the hydrocarbon species formed in the reactor: styrene ($C_6H_5C_2H_3$), benzene (C_6H_6), cyclopentadienyl (C_5H_5), vinylacetylene (C_4H_4), and the methyl radical (CH_3) (Figure 3). The reaction apparatus represents a complex multi reaction environment, which is distinctly different from crossed molecular beam experiments. However, valid conclusions on the reaction mechanisms can be made, if we consider various aspects of the experiment. Firstly, we pre-define the location of the radical center to the phenyl radical, from which all subsequent reactions follow. Here, helium seeded vinyl cyanide on its own under the same conditions (300 Torr, 1,000 K) does not break down to the products implying that all reaction products begin from a reaction with the phenyl radical. Secondly, the reaction takes place on the microsecond timescale under a gas expansion.³⁰⁻³² Third, we have a large excess of vinyl cyanide compared to phenyl radicals. With these constraints on the number and type of mechanisms available we present the simplest and most likely reactions that form the products observed. Our considerations of the reactions follow arguments on the availability of reactants and the presence/absence of entrance barriers. Our approach utilizes every product observed, coupled with background knowledge of the reaction mechanisms to derive a global reaction scheme of the experiment. Ellison et al. have elegantly attempted to derive kinetic models of the pyrolytic nozzle, but are unable to gain the necessary accuracy due to the unknown pressure and temperature differentials.³³

The experimental results can be reconciled by contemplating three initial reaction pathways: (i) a hydrogen abstraction by the phenyl radical (C_6H_5) from the α -carbon atom of the vinyl cyanide molecule (C_2H_3CN) forming benzene (C_6H_6) plus the cyanovinyl radical (C_2H_2CN), (ii)

the decomposition of vinyl cyanide ($\text{C}_2\text{H}_3\text{CN}$) to the vinyl radical (C_2H_3) plus the cyano radical (CN), and (iii) the reaction of the phenyl radical (C_6H_5) with vinyl cyanide ($\text{C}_2\text{H}_3\text{CN}$) forming via addition to the α -carbon atom followed by hydrogen atom elimination cinnamon nitrile ($\text{C}_6\text{H}_5\text{CHCHCN}$). Note that hydrogen abstraction reactions of the phenyl radical with unsaturated molecules (i) proceed efficiently at elevated temperatures and lead to the formation of benzene plus the corresponding hydrocarbon radicals;³¹ Wilhelm et al. probed the unimolecular decomposition of vinyl cyanide ($\text{C}_2\text{H}_3\text{CN}$) verifying the cleavage of the weak carbon-carbon single bond in reaction (ii);³⁴ barrier-less phenyl addition - atomic hydrogen elimination reactions such as reaction (iii) were investigated under single collision conditions verifying the formation of phenyl-substituted molecules.^{35,36} Successive reactions of the phenyl radical (C_6H_5) with the cyanovinyl ($\text{C}_2\text{H}_2\text{CN}$), vinyl (C_2H_3), and cyano (CN) radicals can form cinnamon nitrile ($\text{C}_6\text{H}_5\text{CHCHCN}$), styrene ($\text{C}_6\text{H}_5\text{C}_2\text{H}_3$), and benzonitrile ($\text{C}_6\text{H}_5\text{CN}$), respectively; these radical-radical reactions are exoergic by 491 to 555 kJ mol^{-1} and do not involve any entrance barriers. The formation of cyclopentadienyl (C_5H_5), vinylacetylene (C_4H_4), and methyl radicals (CH_3) is associated with the thermal degradation of hydrocarbons.^{30-33, 37}

Considering the molecular formula of the pyridine molecule ($\text{C}_5\text{H}_5\text{N}$), three pathways can in principle synthesize pyridine via reaction of the 1,3-butadiene molecule ($1,3\text{-C}_4\text{H}_6$) with the cyano radical (CN) [1], the reaction of the vinyl radical (C_2H_3) with vinyl cyanide ($\text{C}_2\text{H}_3\text{CN}$) [2], and through the reaction of vinyl cyanide ($\text{C}_2\text{H}_3\text{CN}$) with the cyanovinyl radical ($\text{C}_2\text{H}_2\text{CN}$) [3]. Note that the reaction of the cyano radical with 1,3-butadiene was investigated recently via a crossed molecular beams experiment³⁸ and also computationally.³⁹ The authors concluded that pyridine can be only formed at levels of less than 1 % with the dominating product being the 1-cyano-1,3-butadiene isomer ($\text{C}_2\text{H}_3\text{C}_2\text{H}_2\text{CN}$) (99 %). Since the PIE curve at m/z 79 ($\text{C}_5\text{H}_5\text{N}^+$) can be reproduced with *only* the pyridine isomer and *without* any contribution from the 1-cyano-1,3-butadiene isomer, we determine that in the pyrolytic reactor, pyridine is not formed via the reaction of the cyano radical with 1,3-butadiene. Note that this conclusion is also supported by the absence of any 1,3-butadiene reactant in the pyrolytic reactor. The remaining pathways – the reactions of vinyl cyanide with the vinyl radical (reaction [2]) and with the cyanovinyl radical (reaction [3]) - have neither been explored computationally nor experimentally prior to this study. Therefore, we conducted a systematic electronic structure calculations to compute the relevant stationary points of the underlying potential energy surfaces (PES) (Figure 4).



First, the reaction of vinyl cyanide with the vinyl radical is initiated by the addition of the radical with its radical center to the α -carbon atom of vinyl cyanide forming a $\text{C}_5\text{H}_6\text{N}$ radical intermediate [i1], which is bound by 164 kJ mol^{-1} with respect to the separated reactants; even at the highest level of theory, this initial addition step has a small entrance barrier of about 9 kJ mol^{-1} . This intermediate can either lose a hydrogen atom forming 1-cyano-1,3-butadiene ($\text{C}_2\text{H}_3\text{C}_2\text{H}_2\text{CN}$) (p1) through a tight exit transition state in an overall exoergic reaction (-24 kJ mol^{-1}) or isomerize via a hydrogen shift to [i2], which in turn can also emit a hydrogen atom forming 1-cyano-1,3-butadiene ($\text{C}_2\text{H}_3\text{C}_2\text{H}_2\text{CN}$) (p1). Alternatively, [i2] undergoes a hydrogen shift to [i4] via a barrier located 44 kJ mol^{-1} above the energy of the separated reactants or ring closes to [i3]. Both [i4] and [i3] can isomerize via ring closure and a hydrogen shift, respectively, to [i5]. The latter can ultimately decompose via hydrogen atom emission forming the pyridine molecule (p2) in an overall exoergic reaction (-119 kJ mol^{-1}). *Second*, the reaction of vinyl cyanide with the cyanovinyl radical is initiated by the addition of the radical center to the α -carbon atom of vinyl cyanide. This process is barrierless leading to intermediate [i6], which undergoes a hydrogen shift forming [i7]. The latter can either emit a cyano radical plus 1-cyano-1,3-butadiene ($\text{C}_2\text{H}_3\text{C}_2\text{H}_2\text{CN}$) (p1) in an overall endoergic reaction ($+50 \text{ kJ mol}^{-1}$) or isomerize via a hydrogen atom shift from the CH_2 group to the carbon next to the nitrogen atom forming [i8], which then can ring close to [i9]. This intermediate either ejects a cyano group or undergoes cyano group migration to reach [i10] or [i11] prior to its elimination yielding pyridine (p2). The overall formation of pyridine is exoergic by 44 kJ mol^{-1} . Note that intermediates i6 and i7 can emit a hydrogen atom forming 1,4-dicyano-1,3-butadiene involving tight exit transition states.

Having identified two possible routes to pyridine formation (Figure 4), we are attempting now to rationalize which is likely to be the predominant reaction pathway in the pyrolytic reactor. *First*, based on the energetics alone, the reaction of the vinyl radical with vinyl cyanide is expected to lead to the formation of two isomers: 1-cyano-1,3-butadiene (p1) and pyridine (p2). However, the transition states involved in the formation of [i4]/[i5] – the crucial reaction intermediate in the formation of pyridine – range 44 kJ mol^{-1} ([i2]→[i4]) and 84 kJ mol^{-1} ([i3]→[i5]) above the energy of the separated reactants. Considering that the transition states for

the atomic hydrogen losses from [i1] and [i2] leading to the formation of 1-cyano-1,3-butadiene are close to the energy of the separated reactants and hence well *below* the aforementioned transition states, we can conclude that 1-cyano-1,3-butadiene (p1) should present the dominant product in the reaction of the vinyl radical with vinyl cyanide. Since 1-cyano-1,3-butadiene was not observed in our experiment, we can conclude that the reaction of the vinyl radical with vinyl cyanide does not take place in the pyrolytic reactor. *Second*, let us move our attention to the reaction of vinyl cyanide with the cyanovinyl radical. Here, the formation of the 1-cyano-1,3-butadiene (p1) is strongly endoergic (+50 kJ mol⁻¹) compared to the synthesis of the aromatic pyridine molecule (-44 kJ mol⁻¹). Therefore, based on these energetic considerations alone, we would expect formation of pyridine under our experimental conditions. Recall that the formation of 1,4-dicyano-1,3-butadiene (p3) cannot be excluded since the ionization energy of this isomer of 9.9 eV to 10.1 eV would result in low—if any – data counts close to the ionization energy. Therefore, we propose that the reaction of vinyl cyanide with the cyanovinyl radical may lead to pyridine. This synthesis is governed by an initial addition of the cyanovinyl radical to vinylcyanide followed by hydrogen migration, cyclization, and cyano radical loss to pyridine.

6. Discussion

We have presented evidence of formation of the aromatic pyridine molecule within the pyrolytic reactor at 1,000 K from reactions of the cyano vinyl (C₂H₂CN) radical with vinyl cyanide (C₂H₃CN). We have rationalized the reaction mechanism to proceed via hydrogen abstraction by the phenyl radical from vinyl cyanide to create a cyano vinyl radical (C₂H₂CN) which subsequently reacts with vinyl cyanide (C₂H₃CN) without an entrance barrier to form the product pyridine through hydrogen atom emission in an exothermic reaction. We shall now discuss the implications of facile formation of pyridine to interstellar environments such as cold molecular clouds and circumstellar envelopes of carbon stars.

Firstly, we observe formation of pyridine at temperatures of 1000 K which are also present in carbon-rich circumstellar envelopes close to the photosphere. Here, rich chemistries are expected, particularly involving organic and nitrogen bearing molecules such as vinyl cyanide. Despite the role of circumstellar envelopes as molecular factories, the most important finding we observe is the lack of an entrance barrier to addition of the cyano vinyl radical to vinyl cyanide. Here, the lack of an entrance barrier to reaction implies the reaction is able to operate at low temperatures

like those within cold molecular clouds as well such as the Taurus Molecular Cloud (TMC-1). Here, the low temperatures of the molecular clouds of typically 10 K would not inhibit the formation of pyridine since there is no entrance barrier to overcome.⁴⁰

Since the reaction to the 1-cyano-1,3-butadiene isomer is too endoergic (+50 kJ mol⁻¹) compared to the synthesis of the aromatic pyridine molecule (-44 kJ mol⁻¹), we can conclude that the pyridine molecule can be easily formed in circumstellar envelopes of carbon-rich Asymptotic Giant Branch (AGB) stars. These environments exhibit a rich nitrogen chemistry leading to the formation of hydrogen-deficient, nitrogen-bearing molecules among them vinyl cyanide holding significant fractional abundances with respect to molecular hydrogen of several 10⁻⁹ in the circumstellar envelope of IRC+10216^{9, 14, 15, 41, 42} In these high temperature environments, the radical chemistry can be initiated by hydrogen abstraction processes⁹⁻¹¹ from, for instance, vinylcyanide as detected in the circumstellar envelope of IRC+10216.¹⁵ This process can form the cyano vinyl radical (C₂H₂CN), which then reacts with vinyl cyanide to form pyridine observed in the present experiments mimicking the high temperature conditions in IRC+10216.

7. Conclusions

To conclude, we have established that the aromatic pyridine molecule – the key building block of nitrogenated polycyclic aromatic hydrocarbons (NPAHs) - can be formed via the gas phase reaction of vinyl cyanide with the cyanovinyl radical at both elevated temperatures and low temperatures as found in cold molecular clouds. The documented synthesis of the simplest nitrogen-bearing aromatic molecules via a bimolecular neutral – neutral reaction represents the first step toward a systematic understanding of how complex nitrogen-bearing polycyclic aromatic hydrocarbons such as (iso)quinoline and related molecules could be formed in circumstellar envelopes of carbon stars such as IRC+10216 or in cold molecular clouds like TMC-1. Since the hydrogen atom(s) in vinyl cyanide and in the cyanovinyl radical reactant might be substituted by organic side groups such as by alkyl chains, the reaction of vinyl cyanide with the cyanovinyl radical presents *the* simplest representative of a novel reaction class in which aromatic molecules, where the nitrogen atom is incorporated *within* the aromatic ring, can be formed from readily abundant acyclic precursors such as vinyl cyanide and its fragments in

circumstellar envelopes and the cold molecular clouds. Pyridine could be the central building block to more complex NPAHs: exposed to photons from the central star, pyridine can be photolyzed to form pyridyl radicals (C_5H_4N) via atomic hydrogen loss.⁴³ The pyridyl radical (C_5H_4N) is isoelectronic to the phenyl radical (C_6H_5), which in turn has been demonstrated to synthesize polycyclic aromatic hydrocarbons such as naphthalene ($C_{10}H_8$) and their derivatives via barrier-less neutral-neutral reactions even at temperatures characteristic of molecular clouds as low as 10 K.⁴⁴⁻⁴⁷ Consequently, successive reactions of the isoelectronic pyridyl radicals may even lead to complex NPAHs such as (iso)quinoline in cold molecular clouds thus propagating the incorporation of nitrogen atoms in high molecular weight NPAHs. Here, the infrared spectra of almost all objects in space depict emission bands at 3.3, 6.2, 7.7, 11.2, and 12.7 μm , which are attributed to ultra violet-pumped infrared fluorescence by a population of PAHs with more than 50 carbon atoms.⁴⁸ However, the interstellar 6.2 μm band occurs at too short a wavelength compared to recent matrix isolation studies and computations of these species. One leading explanation for this discrepancy is the presence of complex nitrogen-substituted PAH structures.⁴⁹ Once synthesized in the interstellar medium, at least a fraction of the NPAHs survives subsequent potential photo processing and are incorporated into the building materials for Solar Systems as demonstrated through the identification of NPAHs such as (iso)quinoline together with their alkyl-substituted counterparts in the Murchison and Lonewolf Nunataks 94102 meteorites.^{3, 50} Consequently, the search for interstellar pyridine and complex NPAHs present an exceptional challenge potentially via the recently commissioned Atacama Large Millimeter / Submillimeter Array, but would provide unique insights into the interstellar carbon and nitrogen chemistries leading from simple precursor molecules to NPAHs.

Acknowledgments

This work was supported by the Department of Energy, Basic Energy Sciences (DE-FG02-03ER15411) at the University of Hawaii (RIK). This research was also supported by a Postdoctoral Fellow Appointment by the NASA Postdoctoral Program (DSNP) administered by Oak Ridge Associated Universities through a contract with NASA. MA, OK, and TPT and the Advanced Light Source are supported by the Director, Office of Science, Office of Basic Energy Sciences, of the U.S. Department of Energy under Contract No. DE-AC02-05CH11231 through the Chemical Sciences Division.

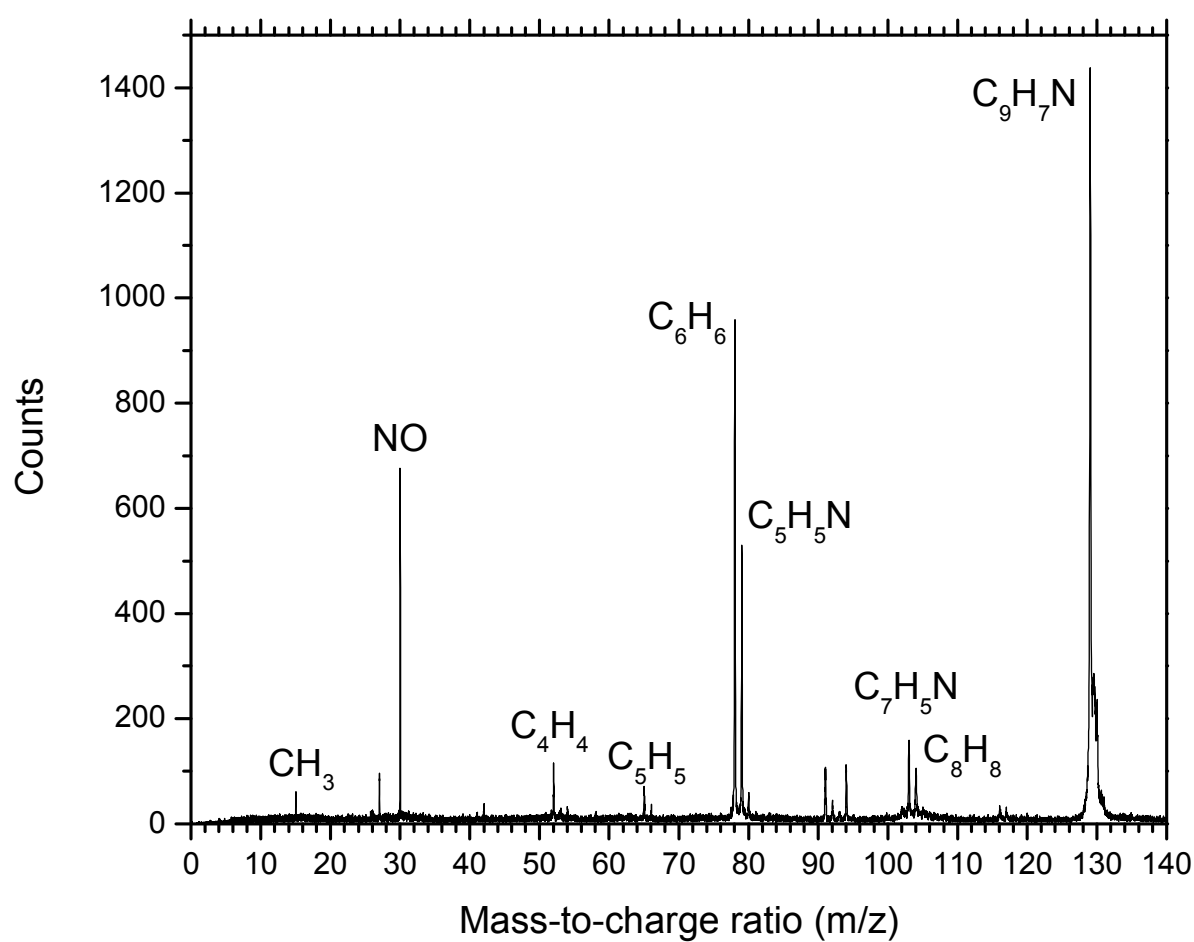


Figure 1: Typical mass spectrum recorded at a photon energy of 10.00 eV and pyrolytic nozzle temperature of 1,000 K.

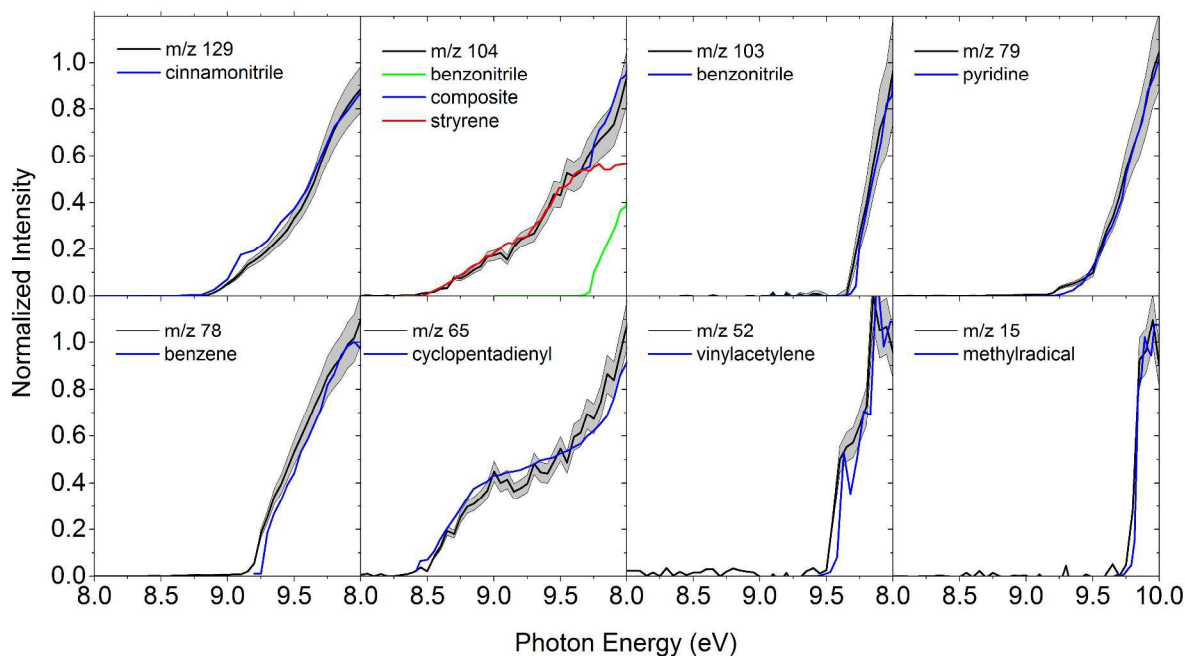


Figure 2: Photoionization efficiency curves (PIEs) at mass-to-charge ratios of m/z 129 (cinnamonnitrile), 104 (benzonitrile,²⁵ styrene²⁴), 103 (benzonitrile²⁵), 79 (pyridine²⁵), 78 (benzene²⁶), 65 (cyclopentadienyl²⁷), 52 (vinylacetylene²⁶), and 15 (methyl radical⁵¹). The experimental PIEs are shown as a black line along with error bars and colored reference PIE(s) together with their linear combination as their composites for m/z 104.

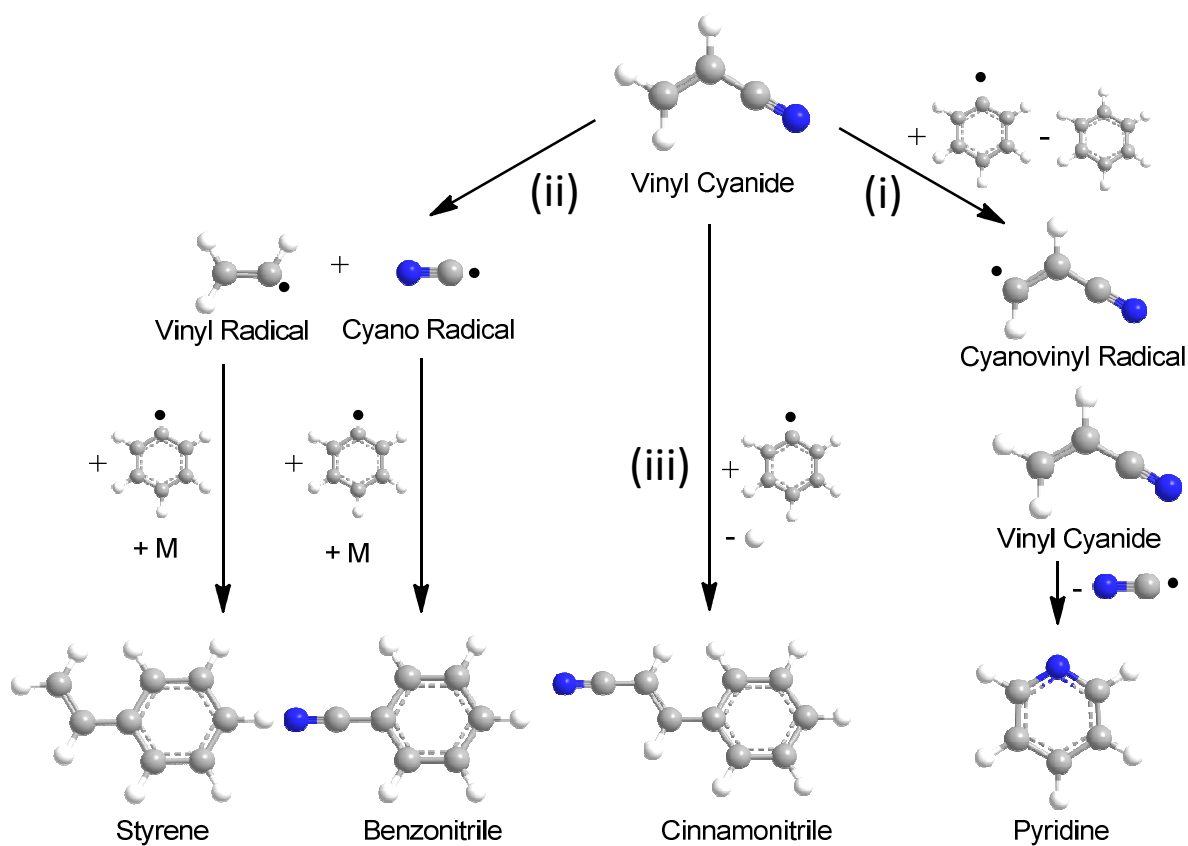


Figure 3: Reaction mechanisms rationalizing the formation of key nitrogen-bearing molecules and styrene produced via reaction of phenyl radicals with vinyl cyanide by exploiting a pyrolysis reactor at a temperature of 1,000 K.

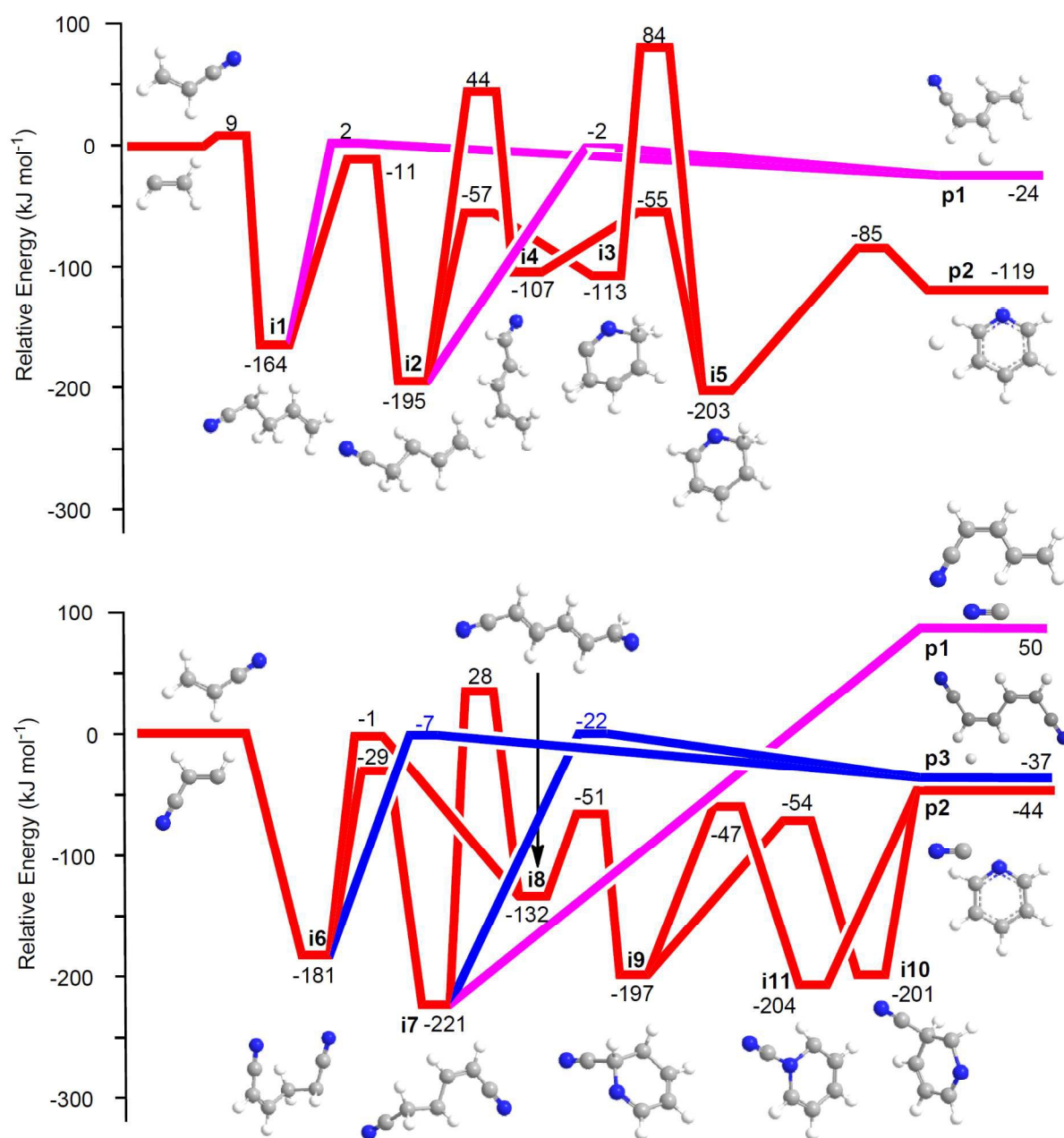
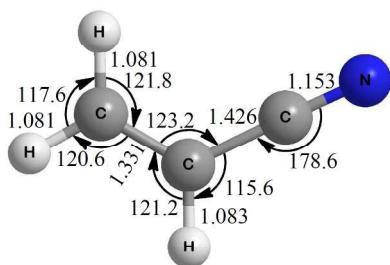
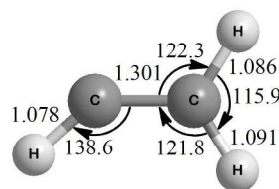
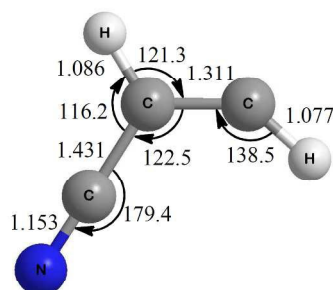
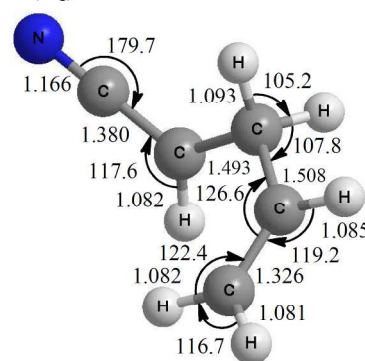
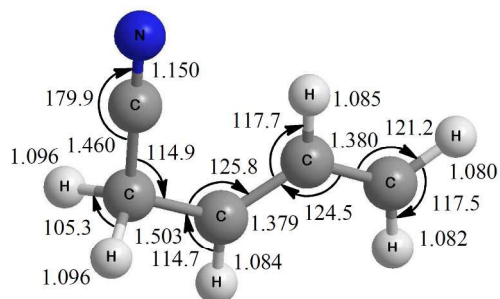
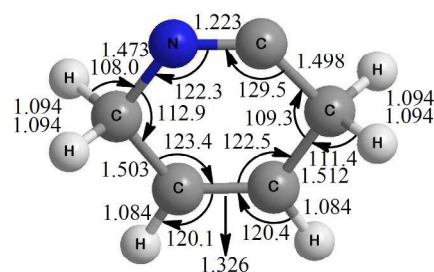
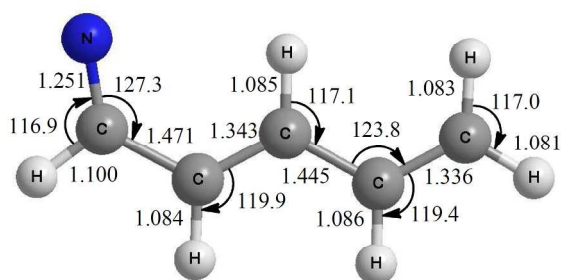
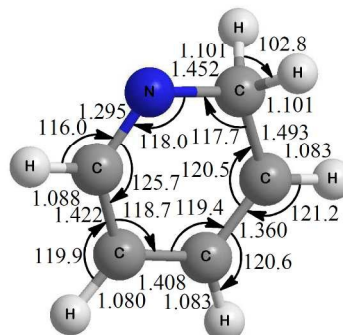
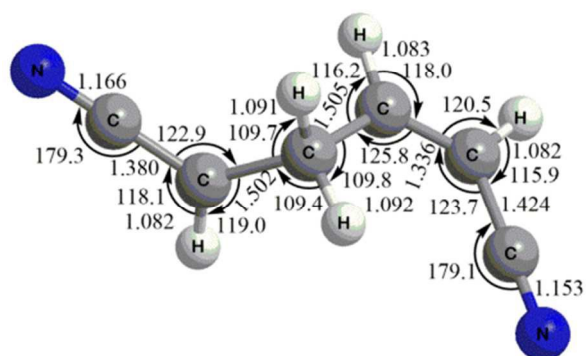
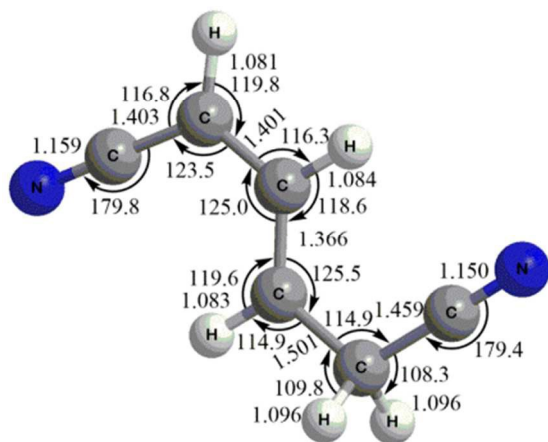
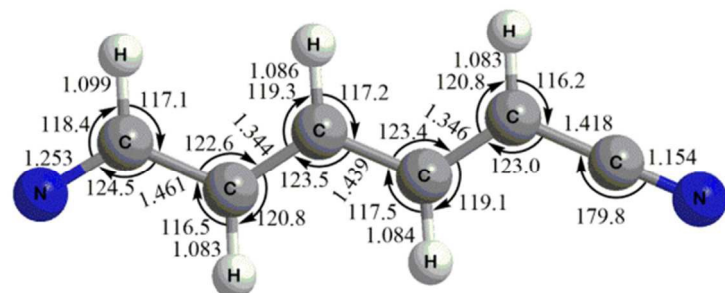


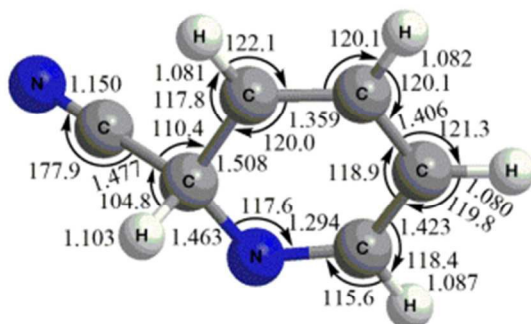
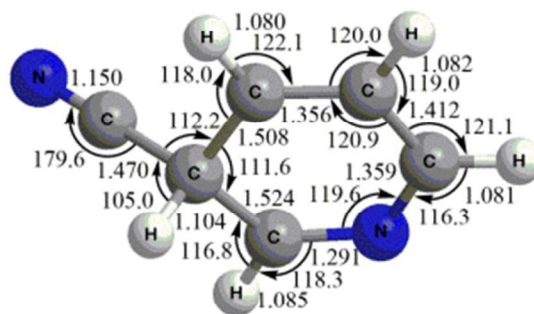
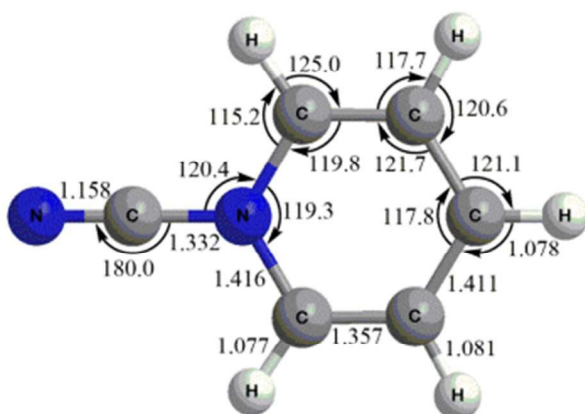
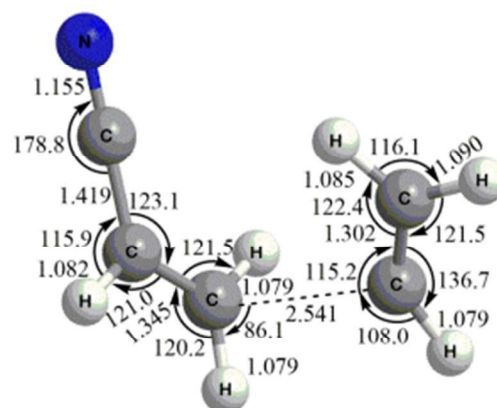
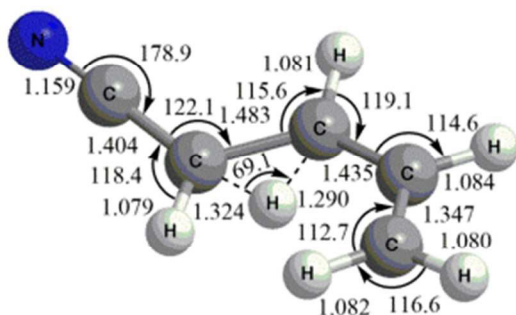
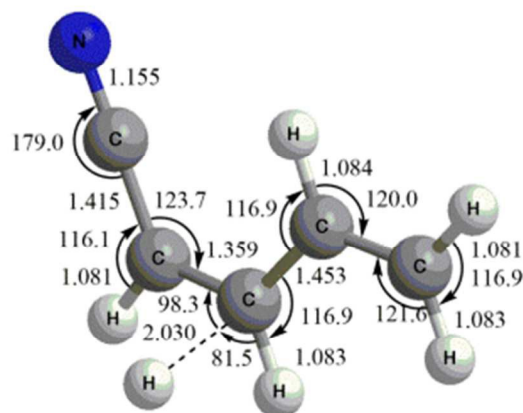
Figure 4: Potential energy surfaces of the reaction of vinyl cyanide with the vinyl radical (top) and with the cyanovinyl radical (bottom). All energies are computed at CCSD(T)/cc-pVTZ level of theory with B3LYP/cc-pVTZ zero-point energy corrections at the B3LYP/cc-pVTZ optimized geometries. All energies are given in kJ mol^{-1} . The red line denotes the most likely pathway to pyridine.

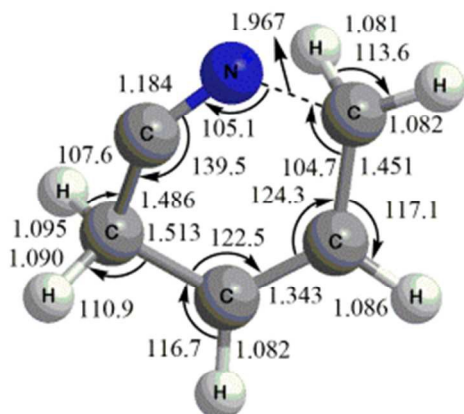
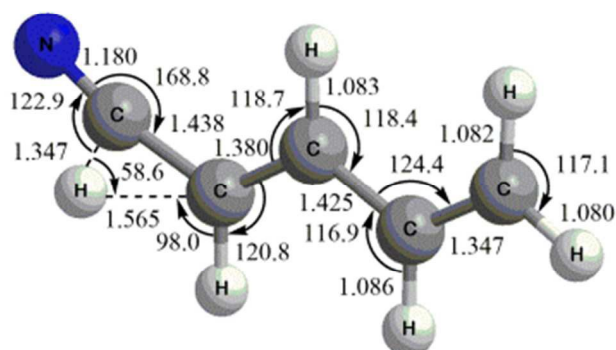
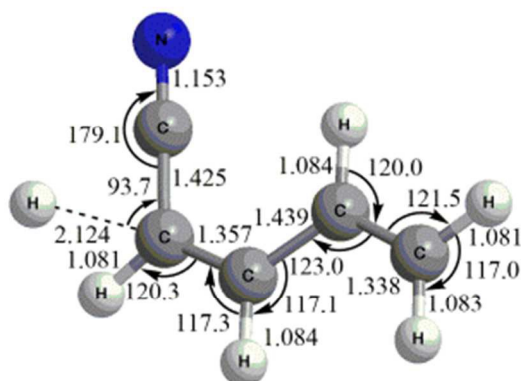
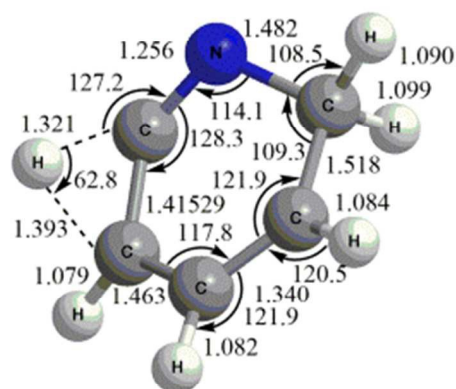
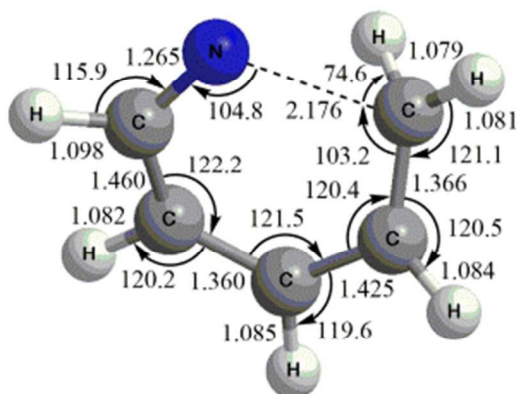
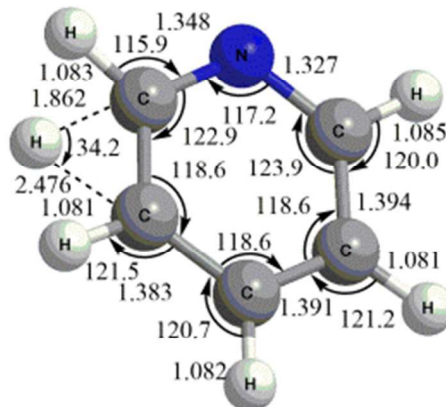
$\text{CH}_2\text{CHCN}(\text{C}_s)(^1\text{A}')$  $\text{CH}_2\text{CH}(\text{C}_s)(^2\text{A}')$  $\text{CHCHCN}(\text{C}_s)(^2\text{A}')$  $\text{i1}(\text{C}_1)$  $\text{i2}(\text{C}_s)$  $\text{i3}(\text{C}_s)$  $\text{i4}(\text{C}_s)$  $\text{i5}(\text{C}_s)$ 

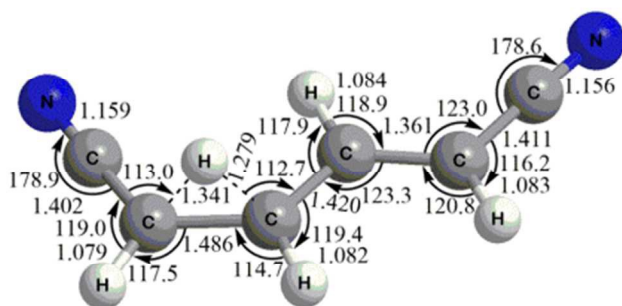
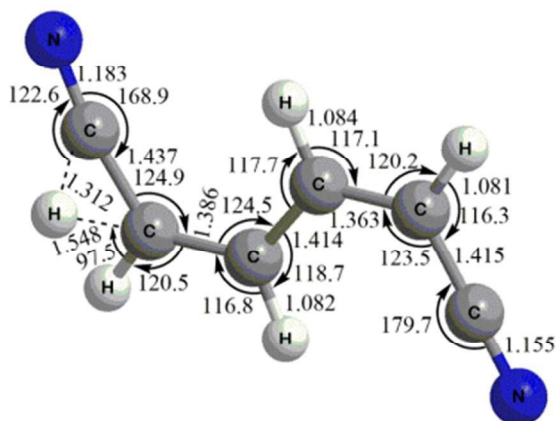
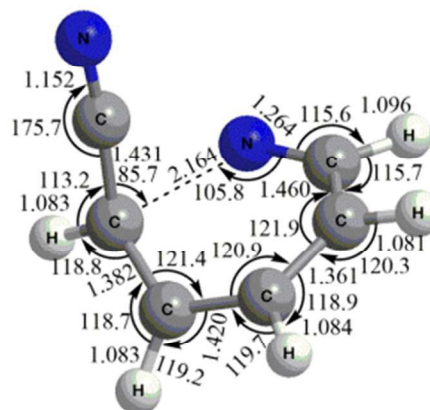
$\mathbf{i6(C_1)}$ 

i7(C_s)

**i8(C_s)**

$$\mathbf{i9(C_1)}$$

$$\mathbf{i10}(\mathbf{C}_1)$$
i11(C_{2v})
$$\mathbf{tsi1}(\mathbf{C}_1)$$

$$\mathbf{tsi1i2}(\mathbf{C}_1)$$

$$\mathbf{tsi1p1}(\mathbf{C}_1)$$


$$\mathbf{tsi2i3(C_1)}$$

$$\mathbf{tsi2i4(C_1)}$$

$$\mathbf{tsi2p1(C_1)}$$
tsi3i5(C₁)tsi4i5(C₁)tsi5p1(C₁)

tsi6i7(C₁)**tsi7i8(C₁)****tsi8i9(C₁)**

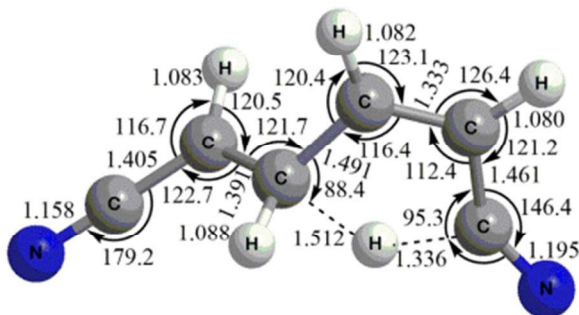
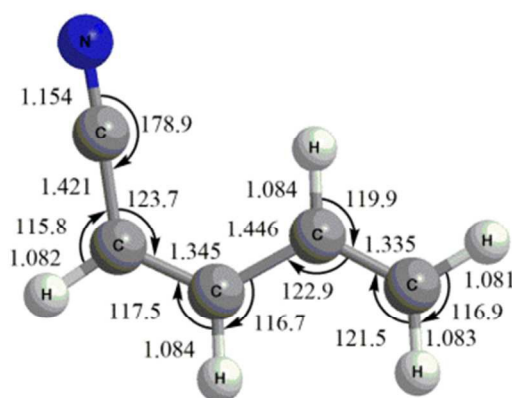
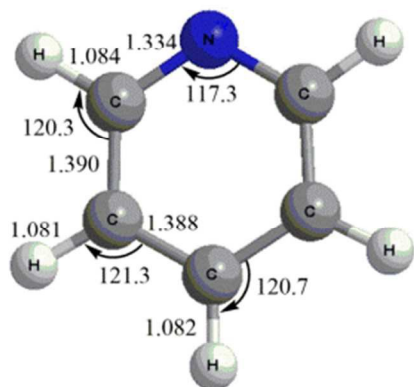
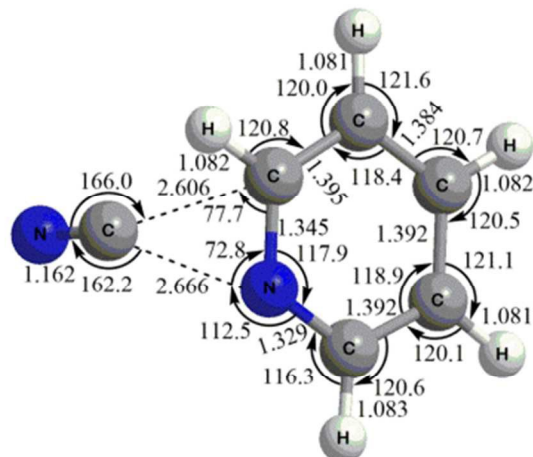
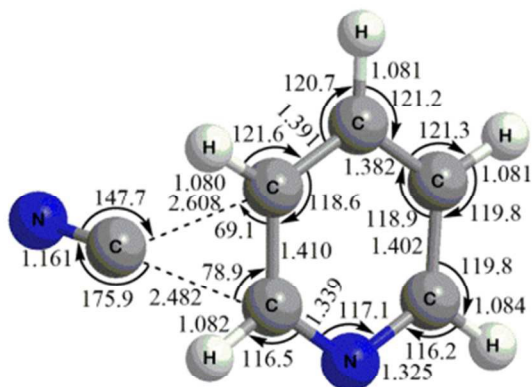


Figure 5. Optimized Cartesian coordinates (distances are given in Å and angles in degrees) of various intermediates, transitions states, and products.

References

1. P. Schmitt-Kopplin, Z. Gabelica, R. D. Gougeon, A. Fekete, B. Kanawati, M. Harir, I. Gebefuegi, G. Eckel and N. Hertkorn, *Proc. Natl. Acad. Sci. U. S. A.*, 2010, **107**, 2763-2768.
2. K. E. Smith, M. P. Callahan, P. A. Gerakines, J. P. Dworkin and C. H. House, *Geochim. Cosmochim. Acta*, 2014, **136**, 1-12.
3. M. P. Callahan, K. Smith, E. H. J. Cleaves, J. Ruzicka, J. C. Stern, D. P. Glavin, C. H. House and J. P. Dworkin, *Proc. Natl. Acad. Sci. U.S.A.*, 2011, **108**, 13995-13998.
4. Z. Martins, O. Botta, M. L. Fogel, M. A. Sephton, D. P. Glavin, J. S. Watson, J. P. Dworkin, A. W. Schwartz and P. Ehrenfreund, *Earth Planet. Sci. Lett.*, 2008, **270**, 130-136.
5. A. S. Burton, J. C. Stern, J. E. Elsila, D. P. Glavin and J. P. Dworkin, *Chem. Soc. Rev.*, 2012, **41**, 5459-5472.
6. R. K. Robins, *J. Am. Chem. Soc.*, 1958, **80**, 6671-6679.
7. S. Pizzarello and W. Holmes, *Geochim. Cosmochim. Acta*, 2009, **73**, 2150-2162.
8. C. S. Contreras, C. L. Ricketts and F. Salama, *EAS Publications Series*, 2011, **46**, 201-207.
9. I. Cherchneff, *EAS Publ. Ser.*, 2011, **46**, 177-189.
10. M. Frenklach and E. D. Feigelson, *Astrophys. J.*, 1989, **341**, 372-384.
11. S. B. Charnley, P. Ehrenfreund and Y. J. Kuan, *Spectrochim. acta. Part A*, 2001, **57**, 685-704.
12. A. Ricca, C. W. Bauschlicher, Jr. and E. L. O. Bakes, *Icarus*, 2001, **154**, 516-521.
13. S. Soorkia, C. A. Taatjes, D. L. Osborn, T. M. Selby, A. J. Trevitt, K. R. Wilson and S. R. Leone, *Phys. Chem. Chem. Phys.*, 2010, **12**, 8750-8758.
14. F. F. Gardner and G. Winnewisser, *Astrophys. J.*, 1975, **195**, L127-L130.
15. M. Agundez, J. P. Fonfria, J. Cernicharo, J. R. Pardo and M. Guelin, *Astron. Astrophys.*, 2008, **479**, 493-501.
16. A. D. Becke, *J. Chem. Phys.*, 1993, **98**, 5648-5652.
17. A. D. Becke, *J. Chem. Phys.*, 1992, **96**, 2155-2160.
18. A. D. Becke, *J. Chem. Phys.*, 1992, **97**, 9173-9177.
19. C. Lee, W. Yang and R. G. Parr, *Physical Review B: Condensed Matter and Materials Physics*, 1988, **37**, 785-789.
20. M. J. O. Deegan and P. J. Knowles, *Chem. Phys. Lett.*, 1994, **227**, 321-326.
21. C. Hampel and K. A. Peterson, *J. Chem. Phys. Lett.*, 1992, **190**, 1-12.
22. P. J. Knowles, C. Hampel and H. J. Werner, *J. Chem. Phys.*, 1993, **99**, 5219-5227.
23. D. W. Kohn, H. Clauberg and P. Chen, *Review of Scientific Instruments*, 1992, **63**, 4003-4005.
24. Z. Zhou, M. Xie, Z. Wang and F. Qi, *Rapid Commun. Mass Spectrom.*, 2009, **23**, 3994-4002.
25. M. Xie, Z. Zhou, Z. Wang, D. Chen and F. Qi, *Int. J. Mass Spec.*, 2011, **303**, 137-146.
26. T. A. Cool, J. Wang, K. Nakajima, C. A. Taatjes and A. McIlroy, *Int. J. Mass Spectrom.*, 2005, **247**, 18-27.
27. N. Hansen, S. J. Klippenstein, J. A. Miller, J. Wang, T. A. Cool, M. E. Law, P. R. Westmoreland, T. Kasper and K. Kohse-Hoinghaus, *J. Phys. Chem. A*, 2006, **110**, 4376-4388.

28. C. A. Taatjes, D. L. Osborn, T. M. Selby and G. Meloni, *J. Phys. Chem. A*, 2008, **112**, 9336–9343.
29. Y. Li, *Photonization Cross Section Database*, <http://flame.nslr.ustc.edu.cn/database/?data=PICS&do=pic&version=en>, 2011.
30. F. Zhang, R. I. Kaiser, A. Golan, M. Ahmed and H. Hansen, *J. Phys. Chem. A*, 2012, **116**, 3541–3546.
31. F. Zhang, R. I. Kaiser, V. V. Kislov, A. M. Mebel, A. Golan and M. Ahmed, *J. Phys. Chem. Lett.*, 2011, **2**, 1731–1735.
32. A. Golan, M. Ahmed, A. M. Mebel and R. I. Kaiser, *Phys. Chem. Chem. Phys.*, 2013, **15**, 341–347.
33. Q. Guan, K. N. Urness, T. K. Ormond, D. E. David, G. B. Ellison and J. W. Daily, *Int. Rev. Phys. Chem.*, 2014, **33**, 447–487.
34. M. J. Wilhelm, M. Nikow, L. Letendre and H.-L. Dai, *J. Chem. Phys.*, 2009, **130**, 044307/044301–044307/044312.
35. D. S. N. Parker, F. Zhang, Y. S. Kim, R. I. Kaiser, A. Landera and A. M. Mebel, *Phys. Chem. Chem. Phys.*, 2012, **14**, 2997–3003.
36. R. I. Kaiser, D. S. N. Parker, M. Goswami, F. Zhang, V. V. Kislov, A. M. Mebel, J. Aguilera-Iparraguirre and W. H. Green, *Phys. Chem. Chem. Phys.*, 2012, **14**, 720–729.
37. D. S. N. Parker, R. I. Kaiser, T. P. Troy, O. Kostko, M. Ahmed and A. M. Mebel, *J. Phys. Chem. A*, 2014, DOI:10.1021/jp509170x.
38. S. B. Morales, C. J. Bennett, S. D. Le Picard, A. Canosa, I. R. Sims, B. J. Sun, P. H. Chen, A. H. H. Chang, V. V. Kislov, A. M. Mebel, X. Gu, F. Zhang, P. Maksyutenko and R. I. Kaiser, *Astrophys. J.*, 2011, **742**, 26–35.
39. B. J. Sun, C. H. Huang, S. Y. Chen, S. H. Chen, R. I. Kaiser and A. H. H. Chang, *J. Phys. Chem. A*, 2014, **118**, 7715–7724.
40. P. Ehrenfreund and S. B. Charnley, *Annual Review of Astronomy and Astrophysics*, 2000, **38**, 427–483.
41. R. L. Pulliam, C. Savage, M. Agundez, J. Cernicharo, M. Guelin and L. M. Ziurys, *Astrophys. J.*, 2010, **725**, L181–L185.
42. N. Balucani, L. Cartechini, A. Bergeat, P. Casavecchia and G. G. Volpi, *EAS Publ. Ser.*, 2001, **496**, 159–162.
43. M.-F. Lin, Y. A. Dyakov, C.-M. Tseng, A. M. Mebel, S. H. Lin, Y. T. Lee and C.-K. Ni, *J. Chem. Phys.*, 2005, **123**, 054309.
44. D. S. N. Parker, F. Zhang, Y. S. Kim, R. I. Kaiser, A. Landera, V. V. Kislov, A. M. Mebel and A. G. G. M. Tielens, *Proc. Natl. Acad. Sci. U. S. A.*, 2012, **109**, 53–58, S53/51–S53/32.
45. R. I. Kaiser, D. S. N. Parker, F. Zhang, A. Landera, V. V. Kislov and A. M. Mebel, *J. Phys. Chem. A*, 2012, **116**, 4248–4258.
46. D. S. N. Parker, B. B. Dangi, R. I. Kaiser, A. Jamal, M. N. Ryazantsev, K. Morokuma, A. Korte and W. Sander, *J. Phys. Chem. A*, 2014, **118**, 2709–2718.
47. T. Yang, L. Muzangwa, D. S. N. Parker, R. I. Kaiser and A. M. Mebel, *Phys. Chem. Chem. Phys.*, 2015, **17**, 530–540.
48. A. G. G. M. Tielens, *Annual Review of Astronomy and Astrophysics*, 2008, **46**, 289–337.
49. D. M. Hudgins, C. W. Bauschlicher, Jr. and L. J. Allamandola, *Astrophys. J.*, 2005, **632**, 316–332.
50. M. A. Sephton, *Nat. Prod. Rep.*, 2002, **19**, 292–311.

51. B. Gans, L. A. V. Mendes, S. Boye-Peronne, S. Douin, G. Garcia, H. Soldi-Lose, B. K. C. de Miranda, C. Alcaraz, N. Carrasco, P. Pernot and D. Gauyacq, *J. Phys. Chem. A*, 2010, **114**, 3237–3246.
52. K. A. Peterson and T. H. Dunning, *J. Phys. Chem.* 1995, **99**, 3898-3901.
53. C. W. Bauschlicher, Jr. and H. Patridge, *J. Chem. Phys.* 1995, **103**, 1788-1791.
54. A. M. Mebel, K. Morokuma, and M. C. Lin, *J. Chem. Phys.* 1995, **103**, 7414-7421.